Applied Clay Science 200 (2021) 105959

Contents lists available at ScienceDirect

Applied Clay Science

journal homepage: www.elsevier.com/locate/clay

Selenium oxyanion exchange with Mg(II)-Fe(III) and Fe(II)-Fe(III) layered double hydroxides

Alexandra E.P. Schellenger [a], Sunho Choi [b], Annalisa Onnis-Hayden [a], Philip Larese-Casanova [a,*]

[a] Department of Civil and Environmental Engineering, Northeastern University, Boston, MA, USA
[b] Department of Chemical Engineering, Northeastern University, Boston, MA, USA

ARTICLE INFO

Keywords:
Selenium
Interlayer anion exchange
Layered double hydroxide
Pyroaurite
Green rust

ABSTRACT

Immobilization of selenium oxyanions from water resources is a helpful strategy to mitigate exposure to Se at concentrations toxic to human and ecosystem health. Pyroaurite-type minerals are layered double hydroxides with high anion exchange capacity with relevance in subsurface environments and applicable to water treatment technologies. Three types of Mg(II)-Fe(III) pyroaurites and Fe(II)-Fe(III) green rusts were evaluated in kinetic studies to determine the influence of different interlayer anions on the uptake of dissolved selenate (SeO_4^{2-}) and selenite ($HSeO_3^-$, SeO_3^{2-}). Selenate and selenite uptake extents with pyroaurites were controlled by the identity of the interlayer anion according to the order $Cl^- > SO_4^{2-} > CO_3^{2-}$, as predicted by known interlayer anion preferences for LDH. The kinetics of Se uptake typically expressed a rapid initial anion exchange step followed by a slow re-exchange back to solution due to competition with expelled interlayer anions. Excess dissolved interlayer anions and high pH values exacerbated this reverse exchange of Se. The results suggest Se oxyanions taken up by pyroaurites may not be firmly sequestered. Selenate uptake by redox-active green rust appears to be subject to the same interlayer anion preference as non-redox active pyroaurite, suggesting that the ability of green rust to reduce selenium oxyanions may be limited by the anion exchange process.

1. Introduction

Selenium (Se) is well-distributed in soils worldwide, and elevated Se levels in seleniferous soils, sediments, and deposits can lead to Se contamination of water resources. Dissolved Se occurs as the oxyanions selenate (SeO_4^{2-}), selenite (SeO_3^{2-}), and hydrogenselenite ($HSeO_3^-$) (the latter two herein collectively referred to as selenite due to their simultaneous presence at the pH values of study), and their toxicity to human and ecosystem health has been established (Lemly, 2002; Lemly, 2004; Painter, 1941). Se concentrations in groundwaters have been found as high as 1 to 6 ppm (Cannon, 1964; Bailey, 2017; Deverel and Millard, 1988) which is far above the WHO maximum guideline value of 10 ppb. To alleviate the problem of Se, water management strategies have focused on promoting Se removal from water to other phases, such as via uptake by plants (Terry et al., 2000; Hansen et al., 1998) in situ reductive precipitation (Morrison et al., 2002; Williams et al., 2013), volatilization to organoselenides (Hansen et al., 1998; Frankenberger and Arshad, 2001), or adsorption to soil components (Hansen et al., 1998; Ford et al., 2007). Water treatment or pollution control technologies also harness adsorption processes for Se removal (Kapoor et al., 1995). Of relevance to both natural and engineered systems are reactive iron minerals which are well-distributed in soils (Cornell and Schwertmann, 2003; Siebecker et al., 2018; Trolard et al., 1997) and can be synthesized to target Se oxyanion sequestration (Tsuji, 2002; Holmes and Gu, 2016).

Pyroaurite and pyroaurite-type minerals are iron-bearing layered double hydroxides (LDH) utilized specifically for their capacity to remove anionic pollutants from water (Goh et al., 2008). Pyroaurite ($Mg^{II}{}_3Fe^{III}(OH)_8[CO_{3\ 0.5}\bullet 2H_2O]$) is constructed of brucite-like sheets of Mg(II)$(OH)_2$ and Fe(*III*)OH_2^+ octahedral sheets, and the layer positive charge is offset by anions occupying the interlayer space along with H_2O (Mills and Christy, 2012). The pyroaurites can form with a variety of different interlayer anions depending on the water chemistry of synthesis or genesis (Bruun Hansen and Koch, 1995; Meng et al., 2004). Because many of these interlayer anions are only weakly bound, the anions are readily exchangeable with solution anions.

The anion exchange capacity of LDH, coupled with thermal stability and high surface area, (Pigna et al., 2016; Sajid and Basheer, 2016) makes these minerals attractive as a potential sorbent for environmentally relevant contaminants. In general, LDH exhibit a preference for

* Corresponding author at: Department of Civil & Environmental Engineering, Northeastern University, 400 Snell Engineering, Boston, MA 02115, USA.
E-mail address: p.laresecasanova@northeastern.edu (P. Larese-Casanova).

https://doi.org/10.1016/j.clay.2020.105959
Received 5 June 2020; Received in revised form 8 December 2020; Accepted 18 December 2020
Available online 30 December 2020

anions in the order of CO_3^{2-} > SO_4^{2-}> OH^-> F^-> Cl^-> Br^-> NO_3^- (Miyata, 1983), an order of highest to lowest charge density as well as highest to lowest binding energies of these anions in the LDH (Li et al., 2006). The ability of LDH to exchange anions of concern in water pollution, including phosphate (Das et al., 2006; Xu et al., 2010; Radha et al., 2005), arsenite and arsenate (Pigna et al., 2016; Xu et al., 2010; You et al., 2001; Yang et al., 2005), chromate (Prasanna and Vishnu Kamath, 2008; Das et al., 2004a; Zhang and Reardon, 2003) nitrate (Sasai et al., 2012), and selenite and selenate (You et al., 2001; Yang et al., 2005; Zhang and Reardon, 2003; Das et al., 2002) has been investigated. Studies suggest that the effectiveness of LDH for adsorbing these anions depends both on environmental conditions (particularly pH and presence and type of competing anions) and on the specific composition of the LDH itself (Goh et al., 2008). The mechanism of exchange may also be influenced by the composition of the LDH sheets (Xu et al., 2010; Radha et al., 2005).

The pyroaurite-type Fe(II)-Fe(III) variety known commonly as green rust has the capability to exchange and reduce anions including nitrate (Hansen et al., 1996; Hansen et al., 2001), chromate (Skovbjerg et al., 2006; Williams and Scherer, 2001), selenate (Schellenger and Larese-Casanova, 2013; Johnson and Bullen, 2003), and hexavalent uranium (O'Loughlin et al., 2003; Latta et al., 2015). The redox capability makes green rust particularly attractive for removing contaminants from water and more firmly immobilizing them through either reductive precipitation (e.g. selenate to elemental selenium (Schellenger and Larese-Casanova, 2013) or transformation to product compounds (e.g. nitrate to ammonium (Hansen et al., 2001)), although its natural occurrence or its engineered utilization can be problematic because green rust itself is less stable than many of its LDH counterparts and rapidly oxidizes in contact with air. Green rusts have been identified within water treatment technologies featuring Fe(0) (Roh et al., 2000; Furukawa et al., 2002). In nature, green rusts may appear as the mineral fougerite (ideally, $[Fe^{II}_4Fe^{III}_2(OH)_{12}][CO_3]\bullet 3H_2O$) within Fe(II)-rich, saturated soils (Trolard et al., 1997; Christiansen et al., 2009; Trolard et al., 2007; Abdelmoula et al., 1998). Chloride green rust (Schellenger and Larese-Casanova, 2013) and sulfate green rust (Johnson and Bullen, 2003) have exhibited different selenate removal kinetic profiles, suggesting interlayer anion identity may also have an influence over selenate uptake, but the carbonate intercalated fougerite variety has not been examined yet.

The LDH most frequently studied for uptake capacity of selenium oxyanions are the Mg-Al (Tsuji, 2002; You et al., 2001; Yang et al., 2005; Das et al., 2004b; Paikaray et al., 2013; Chubar and Szlachta, 2015) and Zn-Al (You et al., 2001; Das et al., 2004a) varieties, and of the Mg(II)-Fe (III) pyroaurites only the carbonate (Das et al., 2002) and sulfate (Paikaray et al., 2013) intercalated versions of Mg-Fe pyroaurites have been examined. Se uptake kinetics have been shown for the carbonate form only, which showed a 2 h approach to equilibrium uptake (Das et al., 2002), and considering carbonate is the most strongly held intercalated anion, other more loosely held anions such as chloride may hold more promise for enhancing Se uptake rate and capacity. Hence, a comparative study of Se uptake kinetics with Mg-Fe pyroaurites with different interlayer anions would be helpful to identify the importance of the interlayer exchange process, especially if different Mg-Fe pyroaurites also hold different specific surface areas that also contribute to uptake extents. Moreover, the interlayer exchange process might be more complicated for Se retention than previously thought. Although rarely documented, there is some evidence that Se oxyanions can be re-exchanged back into solution shortly after uptake by Mg-Al LDH (Yang et al., 2005). LDH are noted to readily exchange anions, and here it is suspected that released interlayer anions may become competitors to Se oxyanions. External competing anions have also been shown to diminish the adsorption capacity of selenate and selenite (You et al., 2001; Yang et al., 2005; Paikaray et al., 2013; Chubar and Szlachta, 2015), however competing anion influences on exchange (and re-exchange) kinetics are hardly documented and require further study.

The purpose of this study is to explore how the anion exchange and re-exchange process influences Se uptake kinetics and how anion identity affects this process for pyroaurites intercalated with Cl-, SO_4^{2-}, or CO_3^{2-}. The four objectives of this work are (i) to describe the dynamics of the anion exchange and re-exchange process, (ii) to evaluate the best pyroaurite mineral for removal of selenate and selenite, (iii), to determine the influence of external anions on the anion exchange and re-exchange kinetics, and (iv) to determine the influence of interlayer anion identity on selenate removal by green rusts. The dynamics of selenate, selenite, and interlayer anion concentrations are tracked within batch reactors, and the water chemistry influences on them are evaluated.

2. Experimental methods

2.1. Mineral synthesis

All chemicals used were of analytical grade, 98–99% purity. Pyroaurite intercalated with carbonate (CO_3-pyr), sulfate (SO_4-pyr), or chloride (Cl-pyr) were synthesized following a modified precipitation method (Meng et al., 2004). A solution of ferric chloride (0.25 M) and magnesium chloride (0.75 M) was added drop wise to a vigorously mixed 250 mL solution containing sodium hydroxide (2 M) and the sodium salt of either carbonate, sulfate, or chloride (0.4 M) until the solution reached pH 9.5. The resulting dispersion of red-brown precipitates was heated for 6 h at 100 °C, after which the solids turned a tan colour, then centrifuged at 10,000 rpm for 10 min to collect the solid. The SO_4-pyr and the CO_3-pyr were each redispersed in a 0.1 M solution of their respective interlayer anion and stirred overnight to remove any remaining interlayer chloride. The solids were washed repeatedly with deionized water by centrifugation, and dried at 70 °C for 24 h. The dry powders were ground with a mortar and pestle, sieved with a 45-μm sieve, and stored dry in the anoxic chamber. The assumed chemical formulas are $Mg^{II}_3Fe^{III}(OH)_8[Cl\bullet 2H_2O]$, $Mg^{II}_3Fe^{III}(OH)_8[SO_{4\ 0.5}\bullet 2H_2O]$, and $Mg^{II}_3Fe^{III}(OH)_8[CO_{3\ 0.5}\bullet 2H_2O]$, based on the initial Mg:Fe synthesis ratios and the suggested number of H_2O for the Cl^- and CO_3^{2-} forms (Anthony et al., 1997).

Carbonate green rust (CO_3-GR) was synthesized by a modified induced hydrolysis method (Taylor et al., 1985) in an anoxic chamber (99%N_2/1%H_2 atmosphere) to avoid contamination from atmospheric carbon dioxide and oxygen. Solutions containing 132 mM $FeCl_2\bullet 4H_2O$ and 27 mM $FeCl_3\bullet 6H_2O$ in 120 mL deoxygenated water were titrated to pH 8 using 1 M Na_2CO_3 under magnetic stirring for 60 min. Solids were filtered by vacuum filtration and appropriate masses were immediately re-suspended in pH 8.0 buffer for batch reactors. Following a similar method, sulfate green rust (SO_4-GR) was synthesized within a 132 mM $FeSO_4\bullet 7H_2O$ and 44 mM $FeCl_3\bullet 6H_2O$ solution in 120 mL deoxygenated water that was titrated to pH 8.0 using 1 M NaOH followed by filtration. Similarly, chloride green rust (Cl-GR) was prepared by titrating a solution containing 66 mM $FeCl_2\bullet 4H_2O$, 22 mM $FeCl_3\bullet 6H_2O$, and 0.5 M NaCl in 120 mL deoxygenated water using 1 M NaOH to pH 8 followed by filtration. All initial Fe(II) concentrations were greater than needed for synthesis in order to keep excess dissolved Fe(II) present to suppress Fe(II) dissolution from GR, thereby helping phase stability. The Fe(II):Fe (III) ratios of the synthesized green rusts were measured colorimetricly as approximately 3.3:1, 2.3:1, and 2.9:1 for CO_3-GR, SO_4-GR, and Cl-GR, respectively, and these values are similar to our prior reports (Schellenger and Larese-Casanova, 2013; Larese-Casanova and Scherer, 2008).

2.2. Experiments

All experiments were conducted within the anoxic chamber. Solutions were prepared using deionized water deoxygenated by autoclaving and equilibration with the anoxic chamber atmosphere. Solution pH was buffered with the Goods buffers 2- ethanesulfonic acid (MES) for pH 6.0, 3-(N-morpholino)propanesulfonic acid (MOPS) for pH 7.0, N-Tris

(hydroxymethyl)methyl-3-aminopropanesulfonic acid (TAPS) for pH 8.0 and 9.0, and N-cyclohexyl-3-aminopropanesulfonic acid (CAPS) for pH 10.0.

Pyroaurite and green rust batch reactors were conducted in polyethylene bottles and homogenized with magnetic stirring. 30 mL solutions of either selenate or selenite were prepared with 20 mM buffer and sampled for initial dissolved selenium concentration. The uptake reaction was initiated by addition of minerals during rapid stirring. 2 mL samples were taken by syringe over the course of 24 h and filtered through 0.2 μm syringe tip filters. Experimental variables for pyroaurite experiments included mineral mass (0.3–1.6 g L^{-1}), solution pH (6–10), initial selenium concentration (0.025–10 mM), and competing anion concentration (0–100 mM of either Cl^- or SO_4^{2-}). Most experiments were conducted with 1.0 g L^{-1} pyroaurite concentrations so that the initial concentration of Se oxyanions (1.0 mM) was not limited by the concentration of available interlayer sites (3.06 mM, 1.56 mM, and 1.48 mM for Cl-pyr, SO_4-pyr, and CO_3-pyr, respectively). Green rust experiments were conducted only with selenate, only at pH 8.0, and with either no competing anion or with a 10 mM concentration of competing anion (either Cl^-, SO_4^{2-}, or CO_3^{2-}).

2.3. Analytical Measurements

Mineral characterization was performed using X-Ray diffraction (XRD) on a Rigaku Ultima IV diffractometer operated with Cu Kα radiation (1.5406 Å wavelength), detector slit size of 10 mm, 0.1 degrees per step, and ~ 60 min scan time at room temperature. Single phase Cl-pyr and CO_3-pyr were confirmed, but SO_4-pyr may have some Cl-pyr impurity (Fig. S1 in the Appendix). Unit cell parameters (*a* and *c*) of the synthesized and reacted pyroaurites are provided in Table S1 in the Appendix, and these values are similar to those from standard reference specimens. Green rust specimens were applied to support slides within the anoxic chamber and coated with a thin layer of deoxygenated glycerol to slow exposure to O_2 during analysis. The specimens were prepared immediately after synthesis, transported to the XRD within a sealed container, and analyzed immediately. The identities of the three synthesized green rusts were thereby confirmed (Fig. S2). BET specific surface area (SSA) was measured with a Quantochrome Nova 2200e analyzer. SSA values were 18.1 m^2 g^{-1} for Cl-pyr, 14.6 m^2 g^{-1} for SO_4-pyr, and 12.9 m^2 g^{-1} for CO_3-pyr. X-ray photoelectron spectroscopy (XPS) measurements were performed with a Surface Science Instruments SSX-100 ESCA Spectrometer (Cornell Center for Materials Research Shared Facility). The Se3p region was scanned at high resolution (instead of Se3d which overlaps the Fe3p region). All spectra were calibrated to the C1s peak (present as C tape support) at 284.4 eV.

Dissolved selenate, selenite, sulfate, and chloride were quantified using a Dionex DX-120 ion chromatograph with 11 mM Na_2CO_3 eluent at a 1.2 mL min^{-1} flow rate and either a Dionex Ion Pac AS22-fast column or a DionexIon Pac AS9-HC column. Dissolved carbonate concentrations were not measurable due to neutralization by the electrolytic suppressor. Dissolved magnesium concentrations were measured using a Bruker Aurora M90 inductively coupled mass spectrometer (supported by Analytik Jena AG). Total Fe and Fe(II) concentrations in green rust experiments were measured following the spectrophotometric phenanthroline method (Schilt, 1969), using a HACH DR 2700 spectrometer at 510 nm detection wavelength.

3. Results and discussion

3.1. Selenium oxyanion uptake kinetics

A comparison of selenate and selenite uptake between three types of pyroaurite was made to examine Se affinity as a function of pre-existing interlayer anion. The experiments were prepared with three types of pyroaurite (Cl-, SO_4-, and CO_3-pyroaurite) at identical mineral concentration (1 g L^{-1}), pH (8), and selenium oxyanion concentration (1 mM) without the presence of competing anions in solution (Fig. 1). Both Cl-pyr and SO_4-pyr show a rapid uptake of selenate within the first five minutes, followed by a longer equilibration period, during which a small amount of the selenate is released from the solid phase back to the bulk solution in a slowly increasing manner (Fig. 1a). A concomitant release of chloride and sulfate to the dissolved phase was observed to mirror the selenate uptake kinetics, which points to an interlayer anion exchange as the primary uptake mechanism. We posit that over time the dissolved phase develops a simultaneous presence of both selenate and the exchanged interlayer anion and creates a competition that could force Cl^- or SO_4^{2-} to re-exchange back with intercalated selenate. No selenate was taken up on CO_3-pyr after 24 h. For selenite, a similar rapid initial uptake was also observed with Cl-pyr and SO_4-pyr with simultaneous Cl^- and SO_4^{2-} release, respectively (Fig. 1b). Some selenite was gradually taken up by CO_3-pyr. Selenite re-exchange after its uptake was minor for all three pyroaurites.

Unfortunately the kinetic behavior does not lend itself to modeling with conventional models. Kinetics of Se oxyanion uptake on other Mg-Fe pyroaurites in the literature are few (Das et al., 2002), but kinetic profiles showing a rapid initial step is common for Se oxyanions on Mg-Al LDH intercalated with either CO_3^{2-} or Cl^- (You et al., 2001; Yang et al., 2005; Chubar and Szlachta, 2015). In only one other instance was a Se re-exchange behavior apparent after its rapid uptake step, which was for selenite on Mg-Al-CO_3 at pH 5.4 (Yang et al., 2005), but no

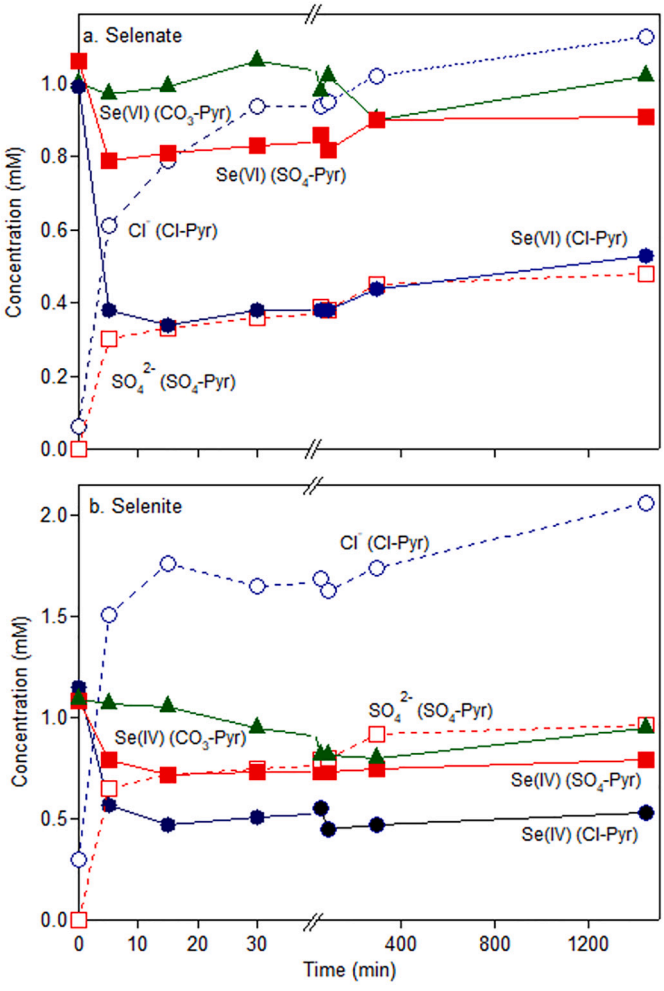

Fig. 1. Kinetics of selenium oxyanion uptake (filled symbols) and interlayer anion release (open symbols) for (a) selenate and (b) selenite on three differently intercalated pyroaurites (circles: Cl-Pyr; squares: SO_4-Pyr; triangles, CO_3-Pyr) with the same mineral mass concentration (1 g L^{-1}) at pH 8.0.

explanation for this non-monotonic uptake behavior was suggested. At times, kinetic behavior was modeled with pseudo-second order kinetics, which is appropriate for sorbate uptake onto a finite number of adsorption sites (Chubar and Szlachta, 2015). Unfortunately, the Se re-exchange observable in Fig. 1 and elsewhere precludes our use of this model.

At the same sorbent mass concentration, the extent of selenate and selenite uptake followed the order of Cl-pyr > SO_4-pyr > CO_3-pyr. This order is the reverse order of interlayer anion preference by LDH, which is governed by anion size and valence charge. The more weakly intercalated Cl^- is more readily exchanged for bivalent selenate and bivalent selenite (selenite, with a pK_{a2} of 8.3, is ~30% SeO_3^{2-} at pH 8.0) which

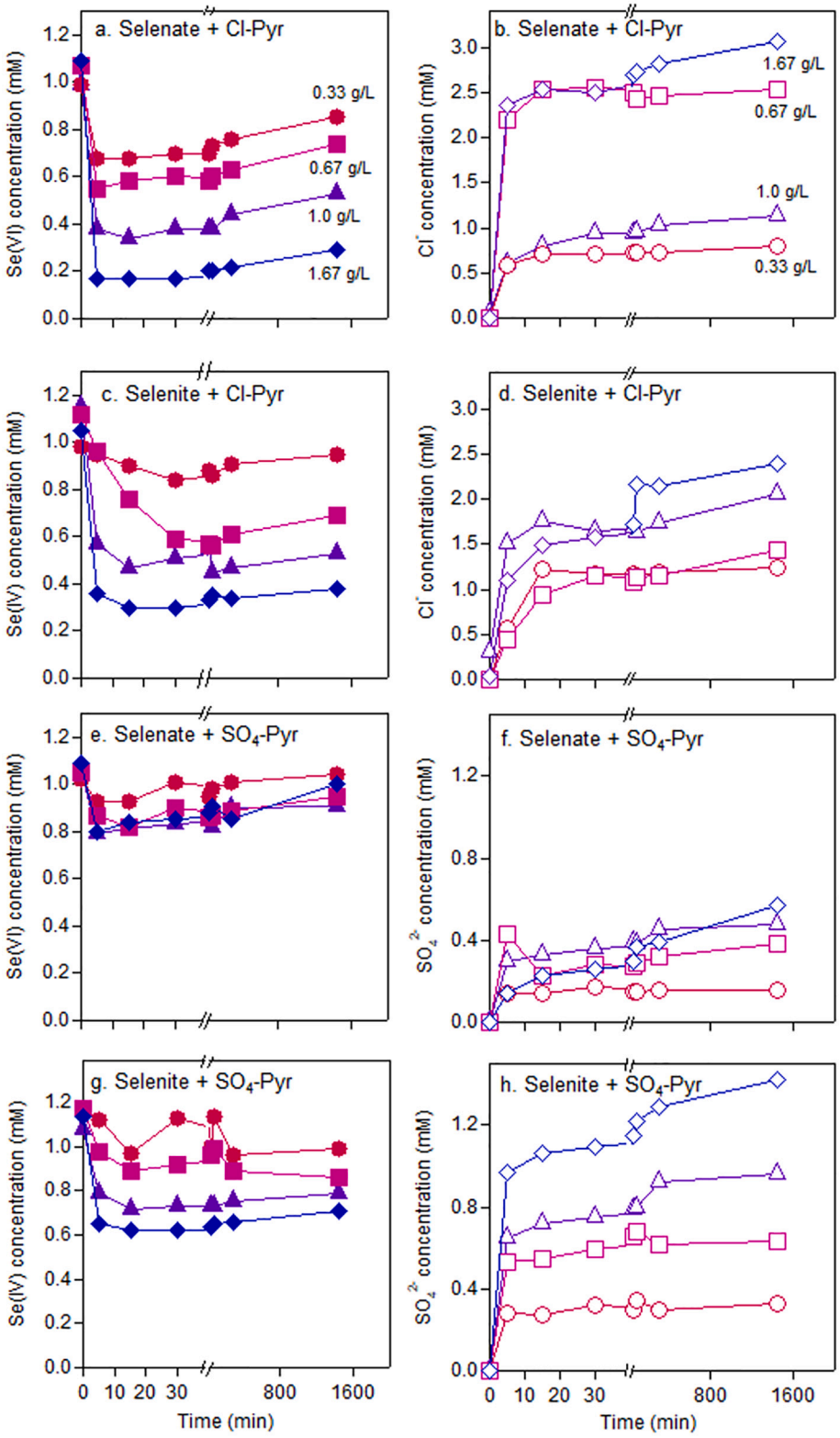

Fig. 2. Kinetics of selenium oxyanion uptake (filled markers) and interlayer anion release (open markers) under varied mineral mass concentrations (circles: 0.33 g L^{-1}, squares: 0.67 g L^{-1}, triangles: 1 g L^{-1}, and diamonds: 1.67 g L^{-1}) for Cl-Pyr (a-d) and SO_4-Pyr (e-h) at pH 8.0.

have greater charge densities compared to monovalent Cl^-. The final amount of Se oxyanions taken up by Cl-pyr was approximately two to three times the amount taken up by SO_4-pyr. Less uptake by SO_4-pyr is expected because, although sulfate and selenate are structurally similar, sulfate is slightly smaller with slightly greater charge density and therefore preferred over selenate. The utter lack of selenate exchange with interlayer carbonate is consistent with LDH having the strongest affinity for carbonate. One possible explanation for some exchange of selenite, but not selenate, with CO_3-pyr is that selenite, with one less O and in a trigonal planar geometry, is smaller than tetrahedral selenate and may therefore fit more easily into the spaces occupied by the small planar carbonate (Sasai et al., 2012). This space constraint by carbonate was also suggested to allow selenite uptake with a Mg-Al LDH with interlayer carbonate, but not selenate or sulfate, which are too large to replace carbonate in the interlayer (Tsuji, 2002).

Experiments with varied LDH concentrations were conducted in order to verify exchange kinetics were reproducible and to gain insight on the processes occurring during anion exchange. First, selenate and selenite uptake kinetics on Cl-pyr and SO_4-pyr again showed a rapid initial uptake, followed by a gradual period of re-exchange, with an accompanying interlayer anion release (Fig. 2). Accordingly, the maximum amount of Se oxyanion taken up was observed within 20 min. CO_3-pyr was not considered due to low uptake capacity and lack of carbonate measurement. Higher pyroaurite mass concentrations resulted in greater selenate and selenite uptake extent, as well as interlayer anion release, due to the greater number of exchange sites provided (Lv et al., 2009). Across all pyroaurite mass concentrations, Cl-pyr took up selenate and selenite at similar extents and to greater extents compared to uptake on SO_4-pyr. SO_4-pyr showed some improved performance for selenite compared to selenate.

Second, the ratio of interlayer anion release to selenium oxyanion uptake in our experiments in Fig. 2 provides further support for interlayer anion exchange in that a sufficient amount of anions exchanged for each selenate or selenite taken up (Table 1). If the amount of anion released to solution had been lower than the amount of selenium anion removed from solution, that would indicate adsorption to surfaces without exchange could be an important process. However, for nearly all Cl-pyr and SO_4-pyr mass concentrations, the amount of anions released was greater than the charge balance required for the amount of selenium taken up. At pH 8, the selenate oxyanion bears a − 2 charge, and based on charge balance we expect an exchange of Cl^- to selenate ratio of 2:1 and SO_4^{2-} to selenate ratio of 1:1. These expected ratios (1.3:1 and 0.7:1, respectively) are slightly smaller for the Se(IV) oxyanions due to less overall charge at pH 8 owing to Se(IV) existing as ~30% selenite (−2) and ~ 70% biselenite (−1). The measured released anion:Se ratios being greater than the expected ratios helps account for Se oxyanion uptake by the interlayer exchange process.

In addition to Se oxyanion exchange into the interlayer, two other processes could be occurring during uptake. First, because more anion release occurred than could be accounted for by Se exchanged, the pyroaurites could spontaneously leak anions alone, despite prior washing with DI water which should have removed any loosely held anions prior to use. The ability of the pyroaurites to leak Cl^- and SO_4^{2-} without exchange were tested in buffered 1.67 g L^{-1} dispersions of Cl-pyr and SO_4-pyr alone without selenium, and up to 0.7 and 1.7 mM of Cl^- and SO_4^{2-} were released, respectively. This leakage could be due to some inherent instability of the pyroaurites within solutions devoid of interlayer anions. Second, a re-exchange, or rebounding, of Se back into the dissolved phase could be occurring after interlayer anions are released. To further test this, experiments were conducted to test the ability of pyroaurite to retain previously intercalated selenate when exposed to other anions. Cl-pyr had previously been reacted with an excess of selenate to make SeO_4-Pyr. Batches of this pyroaurite were then exposed to an excess of Cl^-, SO_4^{2-}, or CO_3^{2-} over 24 h, and the kinetic profile of selenate release into solution is shown in Fig. S3. When exposed to chloride little selenate is released from the pyroaurite initially, and all selenate is re-exchanged into the interlayer by the time the system reaches equilibrium. The presence of both CO_3^{2-} and SO_4^{2-}, however, causes the pyroaurites to exchange selenate permanently with the competing anion. This result suggests that interlayer anions released during Se oxyanion exchange can force a reverse exchange, particularly if the accumulated anions surpass Se oxyanion dissolved concentrations. Furthermore, despite the pyroaurites' ability to bind selenate, subsequent exposure to certain competing anions would reduce the effectiveness of this mineral as a long-term sequesterer of selenium.

The kinetic observations in Figs. 1 and 2 provide information that the interlayer anion exchange process is the governing phase transfer reaction for selenium oxyanions with pyroaurites. Solution-phase dual anion exchange kinetics have also been traced for other LDH including green rusts (Schellenger and Larese-Casanova, 2013; Ayala-Luis et al., 2010) and Cl-pyr (Schellenger and Larese-Casanova, 2013). The replacement of interlayer anions by selenate has also been confirmed in other LDH using XRD by showing a marked increased d-value of the interlayer when the larger selenate anions become intercalated, such as with Fe(II)-Fe(III)-Cl green rust (Schellenger and Larese-Casanova, 2013), Mg(II)-Al(III)-Cl (You et al., 2001), and Mg(II)-Al(III)-CO_3 (Chubar, 2014). Here for Cl-pyr, the replacement of interlayer chloride ions with the larger tetrahedral selenate oxyanions was similarly confirmed within XRD patterns which showed an increase in interlayer space for part of the mineral phase (Fig. S1). The calculated unit cell parameters *a* and *c* for this new SeO_4-pyr phase were similar to those expected for tetrahedral sulfate intercalated SO_4-pyr (Table S1). After selenate uptake with SO_4-pyr, there was no observable change in XRD patterns, likely due to the similar sizes of sulfate and selenate. There was also no observable difference in patterns before and after selenate uptake for CO_3-pyr, but this is likely due to the small amount of selenate uptake. There are previous reports of selenate uptake with Mg(II)-Fe(III)-SO_4 or Mg(II)-Fe(III)-Cl giving only a subtle shift in interlayer space, and their data was interpreted that adsorption to pyroaurite surfaces, in addition to interlayer exchange, was were instead thought to play an important role in selenate uptake (Paikaray et al., 2013). Others have suggested adsorption to surface sites as a removal mechanisms of Se oxyanions with LDH, based on observations of outer-sphere surface complexes by X-ray absorption spectroscopy (Paikaray et al., 2013) or of surface complexes by FTIR spectroscopy (Chubar and Szlachta, 2015; Chubar, 2014). For our pyroaurites, the interlayer anion exchange back to solution and the shifts in reflections for Cl-pyr indicate the interlayer anion exchange process as the primary Se uptake process, although surface adsorption cannot be ruled out as a possibility without spectroscopic measurements.

Table 1
Measured ratios of dissolved interlayer anion released and selenium oxyanion taken up after ~24 h reaction between either Cl-Pyr or SO_4-Pyr and either selenate or selenite at pH 8.0. Kinetic profiles are provided in Fig. 2 of the manuscript.

Mass conc. (g L^{-1})	Measured ratios of anion released/Se taken up			
	Cl/Se(VI)	Cl/Se(IV)	SO_4/Se(VI)	SO_4/Se(IV)
0.33	5.6	41.3	16.0	0.4
0.67	7.7	3.3	3.8	2.3
1	2.3	2.8	3.2	3.3
1.67	3.8	3.6	6.3	3.3
Expected ratios:[a]	2	1.3	1	0.7

[a] Expected ratios are calculated based on the following assumptions. Two Cl^- or one SO_4^{2-} should be released for every SeO_4^{2-} taken up to satisfy charge balance in the pyroaurites. The corresponding charge balances when selenite is taken up are calculated based on selenite oxyanions as a mixture of 70% $HSeO_3^-$ and 30% SeO_3^{2-} at pH 8.0.

3.2. Selenium oxyanion uptake isotherms

The apparent greater uptake capacity of Cl-pyr over SO_4-pyr on a

mass basis could be due either to a greater ability to exchange Cl, to greater surface area, or to both. To better define uptake capacity for comparing the two pyroaurites, Se oxyanion uptake was evaluated with uptake isotherms over a wider range of sorbent and sorbate conditions. Isotherms for Cl-pyr and SO_4-pyr for both Se oxyanions are shown in Fig. 3. The data for Cl-pyr with both oxyanions are well described by the Langmuir model:

$$q = \frac{q_{max}\, K_L\, C}{1 + K_L C} \quad (1)$$

where q_{max} is the maximum uptake capacity, and K_L is the uptake affinity coefficient. The Langmuir model assumes that the sorbent possesses a fixed number of homogeneous binding sites for the sorbate, each of which may bind a single sorbate molecule independently. This is appropriate for anion exchange reactions with LDH that have defined interlayer sites, and has been applied previously for both selenium oxyanions and other anions on LDH (Pigna et al., 2016; You et al., 2001; Prasanna and Vishnu Kamath, 2008; Das et al., 2002; Das et al., 2004b; Paikaray et al., 2013; Chubar and Szlachta, 2015). Table 2 summarizes the fitted Langmuir isotherm parameters for Cl-pyr. Cl-pyr has a slightly higher q_{max} for selenate but a higher K_L for selenite. The q_{max} value for selenate (0.83 mmol g-1) is within range q_{max} values reported for Mg(II)-Al(III)-CO_3 (0.50–1.27 mmol g^{-1}) (Chubar and Szlachta, 2015) and greater than that of Mg(II)-Fe(III)-SO_4 (0.55 mmol g^{-1}) (Paikaray et al., 2013). The q_{max} for selenite on Cl-pyr (0.63 mmol g^{-1}) is also similar to those for Mg(II)-Al(III)-CO_3 (0.50–1.27 mmol g^{-1}) (Chubar and Szlachta, 2015), Mg(II)-Fe(III)-CO_3 (0.37 mmol g^{-1}) (Das et al., 2002), and Mg(II)-Al(III)/Zr(III)-CO_3 (0.53 mmol g^{-1}) (Das et al., 2004a), but smaller than that for Mg(II)-Al(III)-Cl (1.52 mmol g^{-1}) (You et al., 2001).

The Freundlich model better described the isotherm behavior for Se oxyanion uptake on SO_4-pyr based on superior correlation coefficient (R^2) values, with the equation

$$q = K_f C^n \quad (2)$$

where K_f, is related to the overall binding capacity of the sorbent, and n describes the heterogeneity of the sorbent. The Freundlich model assumes that an adsorbent has heterogeneous binding sites, that is, some binding sites on an adsorbent are stronger than others and will be occupied first.

SO_4-pyr might hold a distribution of exchange sites here because the interlayer prefers sulfate, selenate, and selenite to roughly similar extents, giving selenate and selenite difficulty in expelling sulfate in some locations. Or, it is possible the released sulfate partially re-exchanges with interlayer Se (Fig. 2) which suppresses the uptake process and in fact slows the asymptotic approach to a Langmuir-type plateau (q_{max}) which might occur at equilibrium-dissolved Se concentrations higher than the range in Fig. 3. This could be an indication that SO_4-pyr has the potential for an overall higher uptake capacity than Cl-pyr for solutions with very high Se concentrations (several mM). The Freundlich isotherm shape has also been appropriate to describe selenate on Mg(II)-Fe(III)-SO_4 (Paikaray et al., 2013) and Mg(II)-Al(III)-CO_3 (Yang et al., 2005).

Although it is not possible to directly compare parameters developed from different isotherm models, some conclusions can be drawn using single point calculations of predicted amounts taken up (q) at the same equilibrium dissolved Se concentration (e.g., C = 0.1 mM) (Table 2),

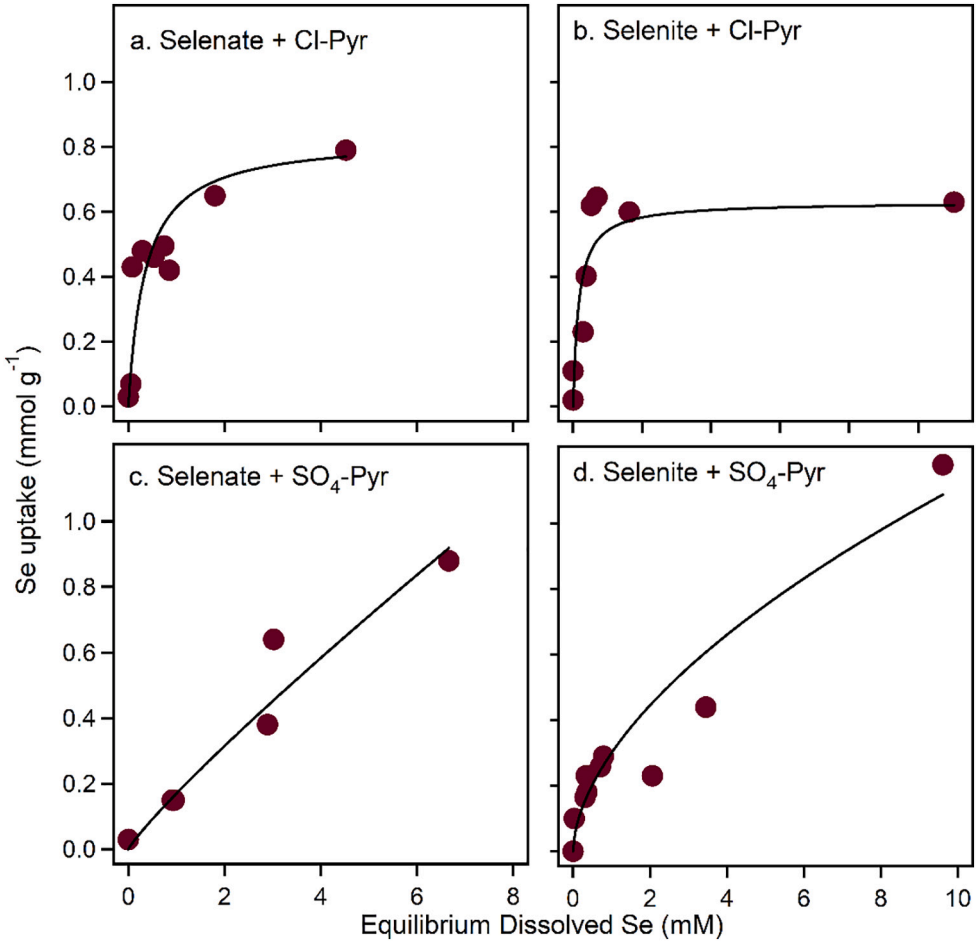

Fig. 3. Isotherms of selenium oxyanion uptake to Cl-Pyr (a, b) and SO_4-Pyr (c, d) at pH 8.0. Data fitting for Cl-Pyr are with the Langmuir model, and fitting for SO_4-Pyr are with the Freundlich model.

Table 2
Summary of modeled isotherm coefficients for selenate and selenite uptake by Cl-Pyr and SO_4-Pyr at pH 8.0.

Sorbent	Sorbate	Langmuir[a]			Freundlich[a]			Estimated q for C = 0.1 mM[b]	
		q_{max}	K_L	R^2	K_F	n	R^2	mmol g^{-1}	mmol m^{-2}
Cl-Pyr	SeO_4^{2-}	0.83	2.76	0.97	0.53	0.38	0.59	0.18	0.010
	SeO_3^{2-}	0.63	8.30	0.99	0.55	0.18	0.23	0.29	0.016
SO4-Pyr	SeO_4^{2-}	6.51	0.02	0.01	0.17	0.93	0.94	0.02	0.001
	SeO_3^{2-}	1.28	0.31	0.52	0.30	0.38	0.82	0.13	0.009

[a] Units for both the Langmuir and Freundlich model coefficients are based on equilibrium aqueous concentration C of mM and sorbed concentration q of mmol g^{-1}.
[b] The estimated sorbed concentration q is calculated for an equilibrium aqueous concentration of 0.1 mM using the Langmuir model for Cl-Pyr and the Freundlich model for SO_4-Pyr.

which allows for quantitatively comparing uptake extent between the two sorbents. These estimated single point q values at $C = 0.1$ mM reveal that uptake extent for selenate and selenite is greater on Cl-pyr compared to SO_4-pyr on a mass sorbent basis. When these q values are normalized to SSA, selenate is taken up 10-fold and selenite nearly 2-fold greater on Cl-pyr compared to SO_4-pyr. This indicates the greater performance of Cl-pyr is not only due to the 24% greater SSA but also mainly to a greater exchange capacity caused by the least preferred interlayer anion. Selenite was also taken up to a greater extent than selenate at this point for both sorbents, and this could be due to the smaller size of selenite compared to selenate which might allow easier or further access within crystallites.

To further check any preference among the Se oxyanions, uptake kinetics were observed for the two pyroaurites with a simultaneous exposure to equimolar (1 mM) selenate and selenite (Fig. S4). Once more, a slight preference to selenite over selenate was observed for both Cl-pyr and SO_4-pyr. These results are not inconsistent with prior modeled rates of selenate and selenite uptake onto Mg(II)-Al(III)-CO_3, which showed similar rates at ~0.12 mM Se concentrations (Chubar and Szlachta, 2015).

3.3. Influence of competing anions

Because released interlayer anions appear to cause re-exchange of previously taken up Se oxyanions, the influence of these anions now initially present in solution was tested for competitive Se oxyanion uptake. For Cl-pyr, selenate and selenite uptake was generally not suppressed over the first ~20 min when chloride concentrations were up to equimolar with initial Se (1 mM) (Fig. 4). However, 1 mM and 10 mM Cl^- resulted in almost complete re-exchange of Se after 24 h, and 100 mM entirely inhibited Se uptake. These results are consistent with prior observations that other dissolved anions start to inhibit Se uptake at initial dissolved anion:Se ratios of about 10:1 (Yang et al., 2005).

Similarly, greater than 1 mM of sulfate also inhibited selenate uptake on SO_4-pyr. Interestingly, selenite exchange with SO_4-pyr was far less sensitive to additional dissolved SO_4^{2-} compared to selenate. The

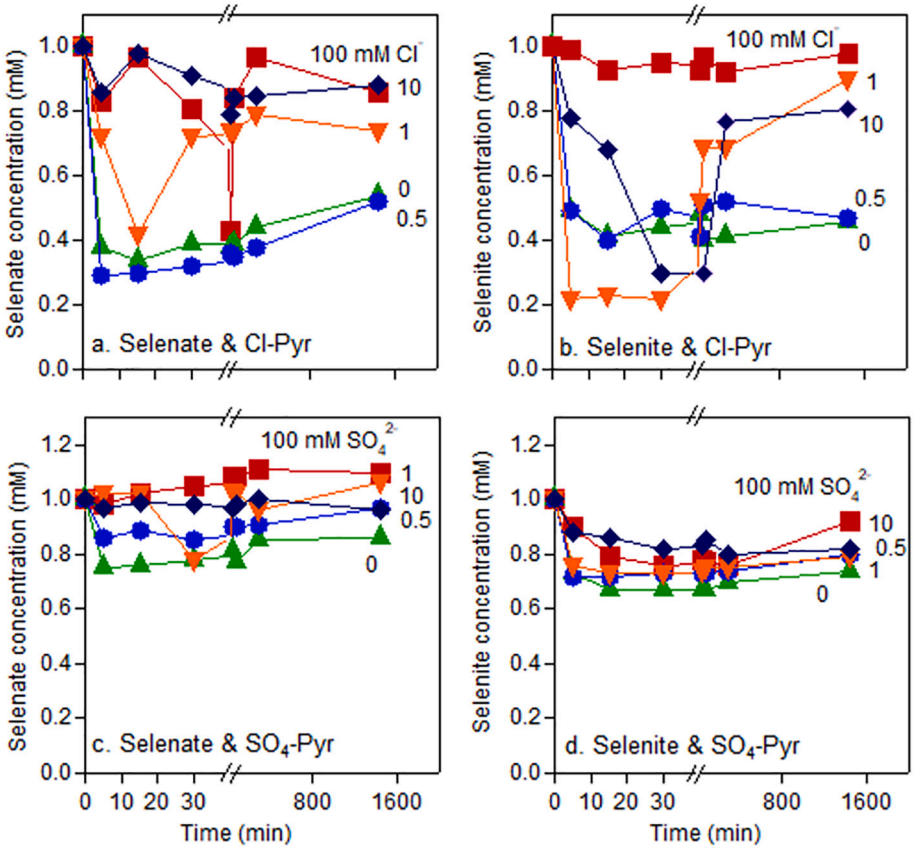

Fig. 4. Kinetics of selenium oxyanion uptake with either Cl-Pyr (a, b) or SO_4-Pyr (1.0 g L^{-1}) in the presence of varied initial competing anion concentration: 0 mM (green triangles), 0.5 mM (blue circles), 1 mM (orange triangles), 10 mM (black diamonds), and 100 mM (red squares). (For interpretation of the references to colour in this figure legend, the reader is referred to the web version of this article.)

insensitivity of selenite to SO_4^{2-} as a competing anion has been observed previously with Mg(II)-Al(III)-CO_3 (Chubar and Szlachta, 2015). This may be due to the ~30% selenite existing as divalent SeO_3^{2-} at pH 8.0 which, being smaller than SO_4^{2-}, has greater charge density than SO_4^{2-} and could possibly be more resistant to re-exchange. Low concentrations of sulfate had a more suppressing effect on selenate than chloride did, which is consistent with the interlayer preference for divalent anions (Miyata, 1983). Overall, Cl-pyr generally out-performed SO_4-pyr and can still be considered a useful exchange medium for Se oxyanions even at some high background electrolyte concentrations so long as exposure to Se is limited to the rapid initial uptake kinetic phase (< ~20 min).

3.4. Influence of pH

Solution pH was varied in order to establish the optimal pH range and to determine if OH^- are competitive anions that can cause Se oxyanion re-exchange. Selenate and selenite uptake kinetics on Cl-pyr and SO_4-pyr showed the rapid initial uptake within the first 10 min followed by varying extents of re-exchange over 24 h depending on solution pH (Fig. 5a-d). pH 8.0 generally held the greatest extent of selenate and selenite removal and showed the least re-exchange, although pH 7.0 also performed well for selenite on SO_4-pyr. At times, nearly all selenate or selenite was re-exchanged at pH 10. The inability for the LDH to retain as much of the oxyanions at pH 10 is in agreement with previous observations that at higher pH more OH^- ions may compete with selenite

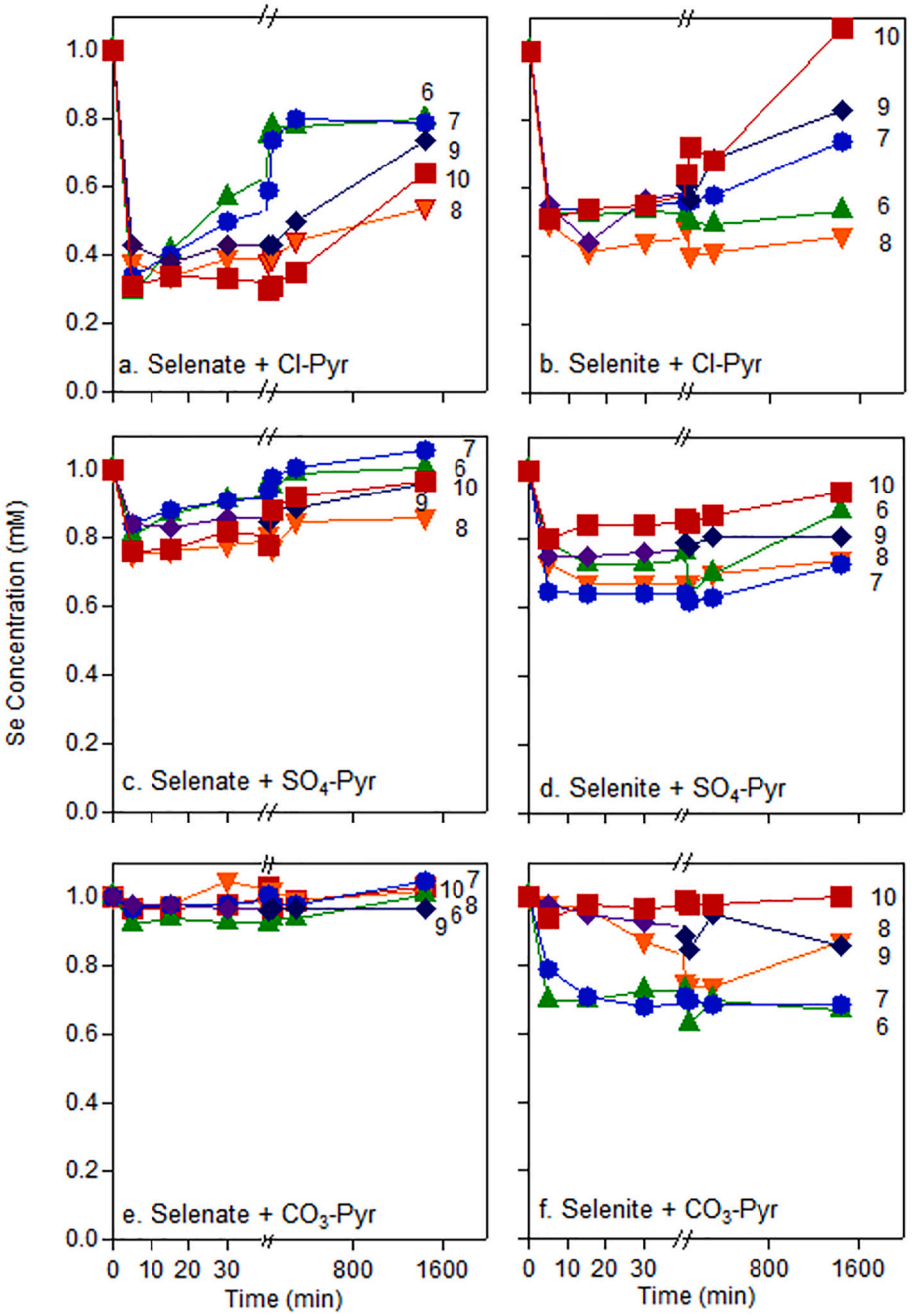

Fig. 5. Kinetics of selenium oxyanion uptake with either Cl-Pyr (a, b), SO_4-Pyr (c, d), or CO_3-Pyr (e, f) (1.0 g L^{-1}) at varied pH: pH 6.0 (green triangles), pH 7.0 (blue circles), pH 8.0 (orange triangles), pH 9.0 (black diamonds), and pH 10.0 (red squares). (For interpretation of the references to colour in this figure legend, the reader is referred to the web version of this article.)

or Cl^- for sites within LDH interlayers (You et al., 2001; Yang et al., 2005; Lv et al., 2009). A possible explanation for the observed reduced exchange capacity of Cl-pyr and SO_4-pyr at lower pH is that the mineral structure becomes less stable and begins to dissolve, reducing the capacity of interlayer sites and releasing competing interlayer anions. To confirm pyroaurite dissolution with pH, measurements of dissolved Mg^{2+} were made after 24 h exposure of Cl-pyr with selenate and show an increase in solution magnesium as pH decreases to 6.0 or 7.0 compared to negligible at pH > 8.0 (Fig. S5). Others have reported metal cation dissolution at lower pH from Mg(II)-Fe(III)-CO_3 (Das et al., 2002), Mg(II)-Al(III)-Cl (You et al., 2001), Zn(II)-Al(III)-Cl (You et al., 2001), Mg(II)-Al(III)-CO_3 (Yang et al., 2005), and Zn(II)-Al(III)-NO_3 (Lv et al., 2009).

Similar to the uptake kinetics in Fig. 1, CO_3-pyr showed almost no reaction with selenate at any pH value, with nearly all sorbed selenate rebounded by 24 h (Fig. 5e). Interestingly, selenite uptake on CO_3-pyr did improve with lower pH with a maximum removal at the lowest pH 6.0 and 7.0 (Fig. 5f). This trend was previously observed for selenite with another Mg(II)-Fe(III)-CO_3, with the reason given that selenite adsorption to surface sites governs uptake, and greater electrostatic attraction occurs when the surfaces become more positive at lower pH (Das et al., 2002). Whether selenite adsorbs on our CO_3-pyr surface sites is unconfirmed. Also, selenite exchange with interlayer carbonate was not confirmed due to lack of dissolved carbonate measurement. Nevertheless, selenite might more readily exchange at lower pH if interlayer CO_3^{2-} near edges protonates to HCO_3^- and H_2CO_3 at pH 6.0–7.0 and would offer less resistance to exchange with $HSeO_3^-$. Despite some uptake of selenite by CO_3-pyr, greater selenite uptake was observed for Cl-pyr at circumneutral pH.

3.5. Selenium oxyanion uptake with three green rusts

The kinetic observations, interlayer anion preference, and the anion competition observations for the pyroaurites were extended to green rusts, the Fe(II)-Fe(III) analog to Mg(II)-Fe(III) pyroaurites. Green rusts are known to exchange their interlayer anions for selenate and slowly reduce selenate to Se(0) via electron transfer from structural Fe(II), but so far, only Cl-GR (Schellenger and Larese-Casanova, 2013) and SO_4-GR (Johnson and Bullen, 2003) reaction with selenate have been reported, and with vastly different Se uptake kinetics. For our solution conditions, selenate uptake increased for the order Cl-GR > SO_4-GR > CO_3-GR when approximately the same amount of total Fe(II) is present (~50 mM) (Fig. 6). This order is the same as for the pyroaurites, which indicates interlayer anion preference also governs selenate removal from water by green rusts. A dried green rust with chloride interlayer was also found to have the fastest removal kinetics, on a green rust mass basis, for chromate (Bond and Fendorf, 2003).

The release of Cl^- and SO_4^{2-} followed selenate uptake for Cl-GR and SO_4-GR, respectively, confirming an interlayer exchange reaction. The rapid selenate uptake and Cl^- release kinetics for Cl-GR were identical to our previous work at higher (10 mM) selenate concentrations (Schellenger and Larese-Casanova, 2013). Cl-GR does not display the gradual re-exchange of selenate that characterized the equilibration of the Cl-Pyr between 2 and 24 h, and instead slowly and continuously decreased, likely due to intercalated selenate being reduced to Se(0) instead of leaking out. The formation of Se(0) after selenate reaction with Cl-GR was previously confirmed by XRD (Schellenger and Larese-Casanova, 2013). Here, Se(0) was also confirmed as the Se product after selenate reaction with SO_4-GR and CO_3-GR by XPS (Fig. S6). For both GRs, two peaks were identified as the Se(0) $3p_{3/2}$ (161.2 and 161.1 eV for SO_4-GR and CO_3-GR, respectively) and the Se(0) $3p_{1/2}$ (166.9 and 166.8 eV) doublet peaks, which have also been observed at or close to these binding energies for Se(0) formed after reduction of selenate by zero-valent iron (Gui et al., 2015; Sasaki et al., 2008). The Se(0) $3p_{1/2}$ peak, though, may overlap a signal of selenate adsorbed to mineral surfaces, previously shown to occur at slightly lower binding energy

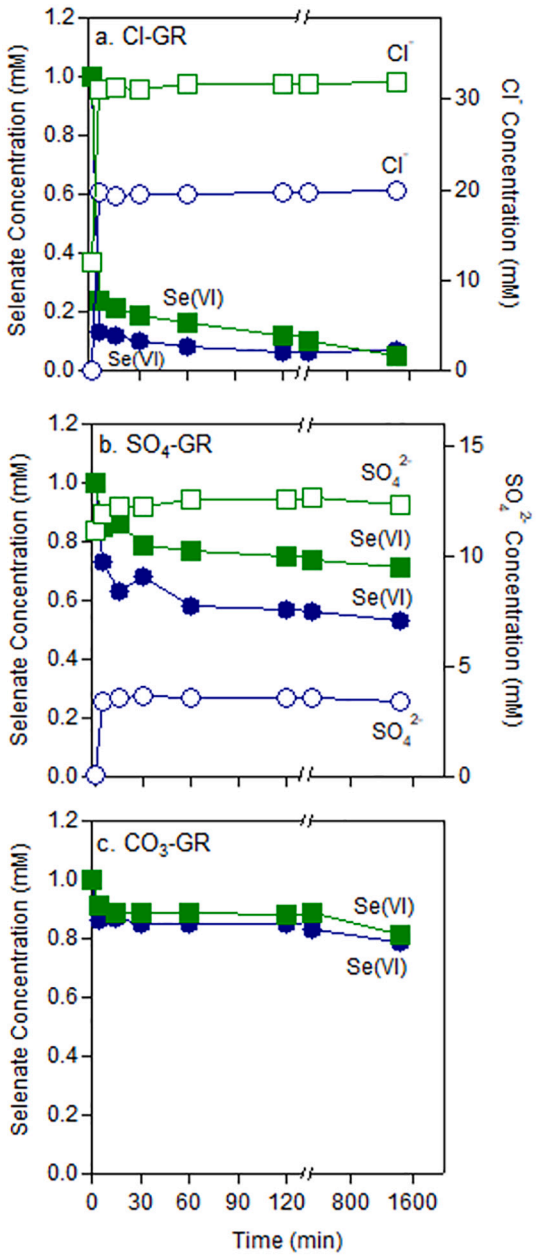

Fig. 6. Kinetics of selenate uptake with either Cl-GR (a), SO_4-GR (b), or CO_3-GR (c) with either no competing anion (circles) or with 10 mM competing anion added (identical to the intercalated anion of the present green rust) (squares). Filled markers represent selenate, and open markers represent the competing or released interlayer anion. Carbonate was not measured in (c). Solution pH was 8.0, and initial green rust concentrations were ~ 50 mM total Fe(II) for all batch reactors. (For interpretation of the references to colour in this figure legend, the reader is referred to the web version of this article.)

(166.26 eV) for selenate adsorbed onto iron oxides (Gui et al., 2015). Here, the starting Na_2SeO_4 salt did produce a peak at 164.8 eV, which is close to a reported value of 164.4 eV (Sartz et al., 1971). This confirmed no peak overlapping the Se(0) $3p_{3/2}$ peak, supporting Se(0) formation only after reduction by GR. Finally, the SO_4-GR and CO_3-GR solids after reaction with selenate were digested with 1 M HCl at room temperature which dissolved Fe but left a red precipitate indicative of Se(0).

On SO_4-GR, selenate also exhibited the rapid initial uptake followed by slower uptake kinetics, which is consistent with the Cl-pyr here but different than the SO_4-GR used in a prior work (Johnson and Bullen, 2003) that showed a zero-order or even first-order selenate removal over

several hours. Possible reasons for their slower kinetics compared to Fig. 6 are their use of lower selenate concentrations (<50 μM), lower GR concentrations, and potential excess dissolved SO_4^{2-} which might limit selenate uptake.

Whether excess dissolved anions can interfere with selenate removal by green rusts was also tested. The presence of 10 mM excess dissolved Cl^- had only minor influence on selenate exchange rate and no effect on the extent of selenate removal. A 10:1 ratio of Cl^-:SeO_4^{2-} was not sufficient to inhibit selenate uptake, but higher ratios might. Excess 10 mM sulfate resulted in approximately 50% less uptake extent and allowed a gradual reduction of selenate over time, but did not completely prevent selenate uptake as occurred on SO_4-pyr alone. CO_3-GR showed little uptake of selenate, whether excess carbonate was present or not. These results with excess anions indicate that although the interlayer anion exchange process for selenate can be slowed by excess anions, exposed Fe(II) at GR surfaces are still capable of removing selenate in a second removal process.

The identity of green rusts is controlled by the predominant anion present during formation. Consequently, anoxic, Fe(II)-rich waters enriched in sulfate or carbonate may form SO_4-GR or CO_3-GR, respectively. The excess interlayer anions may diminish the ability to exchange for selenate and could significantly slow selenate reduction by Fe(II) in green rusts, perhaps limiting reactive sites to surfaces or edges rather than interlayers. In nature, green rusts have been observed as the carbonate form, i.e. fougerite (Trolard et al., 1997; Christiansen et al., 2009; Trolard et al., 2007; Abdelmoula et al., 1998), and the dissolved CO_3^{2-} responsible for the mineral formation might impose a kinetic limitation to Se oxyanion transformation, or to other metalloid oxyanions that rely on interlayer exchange with green rusts. If in situ generation of any green rust is possible in a water treatment application, the chloride green rust form should be promoted. Water treatment technologies featuring Fe(II) hydroxides (Zingaro et al., 1997) would do well to apply ferrous chloride salts to avoid stronger influences of sulfate.

4. Conclusions

Selenate and selenite uptake extent by pyroaurites is controlled by the identity of the interlayer anion according to the order Cl-pyr > SO_4-pyr > CO_3-pyr which is the same order of least strongly to most strongly held anion in the interlayer. Interlayer anion exchange was confirmed as an important uptake mechanism for Cl-pyr and SO_4-pyr. The chloride pyroaurite form showed the greatest selenium oxyanion uptake extent both on a mass basis and after considering surface area differences, and should be considered as the preferred pyroaurite form for water treatment applications. The SO_4-pyr used here appears to have a greater uptake capacity at high Se concentrations, but Cl-pyr has greater uptake capacity at lower Se concentrations more relevant to environmental and wastewater conditions. Future work should explore ways to make interlayer sites more available to dissolved Se oxyanions, such as creating nano-sized crystallites of Cl-pyr.

Optimal conditions for their use in treatment technologies can be inferred from the kinetic study. Maximum Se uptake typically occurred within 10 min, but retention was not permanent. Se oxyanion re-exchange back to solution is a process that works against Se uptake with pyroaurites, and it is thought to occur due to both the expelled intercalated anions and excess anions initially present competing with Se for interlayer sites. Here, Se re-exchange can be an overriding process when the concentration of competing anions is greater than Se oxyanion concentration and when pH is 9 or greater. Se uptake with chloride pyroaurite is strongly pH dependent with the optimal solution pH at 8.0. Se uptake kinetics can therefore be more complex than previously realized, and new kinetic models are required to describe both uptake and re-release. Exposure of pyroaurites to Se-laden waters should be limited to the time of the initial rapid uptake step.

In subsurface environments where LDH form, the ambient anions that initially populate interlayer sites might limit LDH uptake of Se oxyanions. The exchange reactions with green rust suggest that the same factors that influence non-redox active LDH may also affect the ability of green rust to exchange for selenate, which in turn impacts the ability of the green rust to reduce and fully immobilize Se oxyanions. The carbonate form of green rust, so far the only green rust form found in nature, showed minimal selenate removal from water.

Declaration of Competing Interest

The authors declare that they have no known competing financial interests or personal relationships that could have appeared to influence the work reported in this paper.

Acknowledgements

The authors thank the Northeastern University Center for Renewable Energy Technology (NUCRET) for XRD access, particularly Sanjeev Mukerjee and Serge Pann. Thanks also go to Kwun Lok Yu and Hope Ianiri for synthesis assistance. This work made use of the Cornell Center for Materials Research Shared Facilities which are supported through the NSF MRSEC program (DMR-1719875). This project was financially supported by the U. S. National Science Foundation (Grant CBET-1236182).

Appendix A. Supplementary data

Supplementary data to this article can be found online at https://doi.org/10.1016/j.clay.2020.105959.

References

Abdelmoula, M., Trolard, F., Bourrie, G., Genin, J.R., 1998. Evidence for the Fe(II)-Fe(III) green rust "fougerite" mineral occurrence in a hydromorphic soil and its transformation with depth. Hyperfine Inter. 112, 235–238.

Anthony, J.W., Bideaux, R.A., Bladh, K.W., Nichols, M.C., 1997. Handbook of Mineralogy, Mineralogical Society of America, Chantilly, VA 20151–1110, USA. http://www.handbookofmineralogy.org/.

Ayala-Luis, K.B., Koch, C.B., Hansen, H.C.B., 2010. Intercalation of linear C9–C16 carboxylates in layered Fe^{II}–Fe^{III}-hydroxides (green rust) via ion exchange. Appl. Clay Sci. 48, 334–341.

Bailey, R.T., 2017. Review: Selenium contamination, fate, and reactive transport in groundwater in relation to human health. Hydrogeol. J. 25, 1191–1217.

Bond, D.L., Fendorf, S., 2003. Kinetics and structural constraints of chromate reduction by green rusts. Environ. Sci. Technol. 37, 2750–2757.

Bruun Hansen, H.C., Koch, C.B., 1995. Synthesis and characterization of pyroaurite. Appl. Clay Sci. 10, 5–19.

Cannon, H.G., 1964. Geochemistry of Rocks and Related Soils and Vegetation in the Yellow Cat Area, Grand County, Utah. United States Geological Survey, Washington, DC (Bulletin No. 1176).

Christiansen, B.C., Balic-Zunic, T., Dideriksen, K., Stipp, S.L.S., 2009. Identification of green rust in groundwater. Environ. Sci. Technol. 43, 3436–3441.

Chubar, N., 2014. EXAFS and FTIR studies of selenite and selenate sorption by alkoxide-free sol–gel generated Mg–Al–CO_3 layered double hydroxide with very labile interlayer anions. J. Mater. Chem. A 2, 15995–16007.

Chubar, N., Szlachta, M., 2015. Static and dynamic adsorptive removal of selenite and selenate by alkoxide-free sol–gel-generated Mg–Al–CO_3 layered double hydroxide: effect of competing ions. Chem. Eng. J. 279, 885–896.

Cornell, R.M., Schwertmann, U., 2003. The Iron Oxides: Structure, Properties, Reactions, Occurrences and Uses, 2nd ed. Wiley-VCH, Weinheim.

Das, J., Das, D., Dash, G.P., Parida, K.M., 2002. Studies on Mg/Fe hydrotalcite-like-compound (HTlc)-I. Removal of inorganic selenite (SeO_3^{2-}) from aqueous medium. J. Coll. Interf. Sci. 251, 26–32.

Das, J., Das, D., Dash, G.P., Parida, K.M., 2004a. Studies on Mg/Fe hydrotalcite-like-compound (HTlc)-II. Removal of chromium (VI) from aqueous medium. Int. J. Environ. Stud. 61, 605–616.

Das, J., Patra, B.S., Baliarsingh, N., Parida, K.M., 2006. Adsorption of phosphate by layered double hydroxides in aqueous solutions. Appl. Clay Sci. 32, 252–260.

Das, N.N., Konar, J., Mohanta, M.K., Srivastava, S.C., 2004b. Adsorption of Cr(VI) and Se (IV) from their aqueous solutions onto Zr^{4+}-substituted ZnAl/MgAl-layered double hydroxides: effect of Zr^{4+} substitution in the layer. J. Colloid Interface Sci. 270, 1–8.

Deverel, S.J., Millard, S.P., 1988. Distribution and mobility of selenium and other trace elements in shallow groundwater of the western San Joaquin Valley, California. Environ. Sci. Technol. 22, 697–702.

Ford, R.G., Wilkin, R.T., Puls, R.W., 2007. Monitored Natural Attenuation of Inorganic Contaminants in Ground Water Volume 2: Assessment for Non-Radionuclides Including Arsenic, Cadmium, Chromium, Copper, Lead, Nickel, Nitrate, Perchlorate, and Selenium. EPA/600/R-07/140.

Frankenberger, W.T.J., Arshad, M., 2001. Bioremediation of selenium-contaminated sediments and water. BioFactors 14, 241–254.
Furukawa, Y., Kim, J., Watkins, J., Wilkin, R.T., 2002. Formation of ferrihydrite and associated iron corrosion products in permeable reactive barriers of zero-valent iron. Environ. Sci. Technol. 36, 5469–5475.
Goh, K., Lim, T., Dong, Z., 2008. Application of layered double hydroxides for removal of oxyanions: a review. Water Res. 42, 1343–1368.
Gui, M., Papp, J.K., Colburn, A.S., Meeks, N.D., Weaver, B., Wilf, I., Bhattacharyya, D., 2015. Engineered iron/iron oxide functionalized membranes for selenium and other toxic metal removal from power plant scrubber water. J. Membr. Sci. 488, 79–91.
Hansen, D., Duda, P.J., Zayed, A., Terry, N., 1998. Selenium removal by constructed wetlands: Role of biological volatilization. Environ. Sci. Technol. 32, 591–597.
Hansen, H.C.B., Koch, C.B., Nancke-Kroge, H., Borggaard, O.K., Sorensen, J., 1996. Abiotic nitrate reduction to ammonium: Key role of green rust. Environ. Sci. Technol. 30, 2053–2056.
Hansen, H.C.B., Guldberg, S., Erbs, M., Bender Koch, C., 2001. Kinetics of nitrate reduction by green rusts—effects of interlayer anion and Fe(II):Fe(III) ratio. Appl. Clay Sci. 18, 81–91.
Holmes, A.B., Gu, F.X., 2016. Emerging nanomaterials for the application of selenium removal for wastewater treatment. Environ. Sci. Nano 3, 982–996.
Johnson, T.M., Bullen, T.D., 2003. Selenium isotope fractionation during reduction by Fe (II)-Fe(III) hydroxide-sulfate (green rust). Geochim. Cosmochim. Acta 67, 413–419.
Kapoor, A., Tanjore, S., Viraraghavan, T., 1995. Removal of selenium from water and wastewater. Int. J. Environ. Stud. 49, 137–147.
Larese-Casanova, P., Scherer, M.M., 2008. Abiotic reduction of hexahydro-1,3,5-trinitro-1,3,5-triazine by green rusts. Environ. Sci. Technol. 42, 3975–3981.
Latta, D.E., Boyanov, M.I., Kemner, K.M., O'Loughlin, E.J., Scherer, M., 2015. Reaction of uranium(VI) with green rusts: effect of interlayer anion. Curr. Inorg. Chem. 5, 156–168.
Lemly, A.D., 2002. Symptoms and implications of selenium toxicity in fish: the Belews Lake case example. Aquat. Toxicol. 57, 39–49.
Lemly, A.D., 2004. Aquatic selenium pollution is a global environmental safety issue. Ecotoxicol. Environ. Saf. 59, 44–56.
Li, H., Ma, J., Evans, D.G., Zhou, T., Li, F., Duan, X., 2006. Molecular dynamics modeling of the structures and binding energies of alpha-Nickel hydroxides and Nickel-Aluminum layered double hydroxides containing various interlayer guest anions. Chem. Mater. 18, 4405–4414.
Lv, L., Sun, P., Gu, Z., Du, H., Pang, X., Tao, X., Xu, R., Xu, L., 2009. Removal of chloride ion from aqueous solution by ZnAl-NO_3 layered double hydroxides as anion-exchanger. J. Hazard. Mater. 161, 1444–1449.
Meng, W., Li, F., Evans, D.G., Duan, X., 2004. Preparation and intercalation chemistry of magnesium–iron(III) layered double hydroxides containing exchangeable interlayer chloride and nitrate ions. Mater. Res. Bull. 39, 1185–1193.
Mills, S.J., Christy, A.G., Génin, J., Kameda, T., Colombo, F., 2012. Nomenclature of the hydrotalcite supergroup: natural layered double hydroxides. Mineral. Mag. 76, 1289–1336.
Miyata, S., 1983. Anion-exchange properties of hydrotalcite-like compounds. Clay Clay Miner. 31, 305–311.
Morrison, S.J., Metzler, D.R., Dwyer, B.P., 2002. Removal of As, Mn, Mo, Se, U, V and Zn from groundwater by zero-valent iron in a passive treatment cell: reaction progress modeling. J. Contam. Hydrol. 56, 99–116.
O'Loughlin, E.J., Kelly, S.D., Cook, R., Csencsits, R., Kemner, K.M., 2003. Reduction of uranium(VI) by mixed iron(II)/iron(III) hydroxide (green rust): Formation of UO_2 nanoparticles. Environ. Sci. Technol. 37, 721.
Paikaray, S., Hendry, M.J., Essilfie-Dughan, J., 2013. Controls on arsenate, molybdate, and selenate uptake by hydrotalcite-like layered double hydroxides. Chem. Geol. 345, 130–138.
Painter, E.P., 1941. The chemistry and toxicity of selenium compounds, with special reference to the selenium problem. Chem. Rev. 28, 179–213.
Pigna, M., Dynes, J.J., Violante, A., Sommella, A., Caporale, A.G., 2016. Sorption of arsenite on Cu-Al, Mg-Al, Mg-Fe, and Zn-Al layered double hydroxides in the presence of inorganic anions commonly found in aquatic environments. Environ. Eng. Sci. 33, 98–104.
Prasanna, S.V., Vishnu Kamath, P., 2008. Chromate uptake characteristics of the pristine layered double hydroxides of Mg with Al. Solid State Sci. 10, 260–266.
Radha, A.V., Vishnu Kamath, P., Shivakumara, C., 2005. Mechanism of the anion exchange reactions of the layered double hydroxides (LDHs) of Ca and Mg with Al. Solid State Sci. 7, 1180–1187.
Roh, Y., Lee, S.Y., Elless, M.P., 2000. Characterization of corrosion products in the permeable reactive barriers. Environ. Geol. 40, 184–194.
Sajid, M., Basheer, C., 2016. Layered double hydroxides: emerging sorbent materials for analytical extractions. TraC-Trend. Anal. Chem. 75, 174–182.
Sartz, W.E., Wynne, K.J., Hercules, D.M., 1971. X-ray photoelectron spectroscopic investigation of Group VIA elements. Anal. Chem. 43, 1884–1887.
Sasai, R., Norimatsu, W., Matsumoto, Y., 2012. Nitrate-ion-selective exchange ability of layered double hydroxide consisting of Mg^{II} and Fe^{III}. J. Hazard. Mater. 215–216, 311–314.
Sasaki, K., Blowes, D.W., Ptacek, C.J., 2008. Spectroscopic study of precipitates formed during removal of selenium from mine drainage spiked with selenate using permeable reactive materials. Geochem. J. 42, 283–294.
Schellenger, A.E.P., Larese-Casanova, P., 2013. Oxygen isotope indicators of selenate reaction with Fe(II) and Fe(III) hydroxides. Environ. Sci. Technol. 47, 6254–6262.
Schilt, A.A., 1969. Analytical Applications of 1,10-Phenanthroline and Related Compounds, 1st ed. Pergamon Press, Oxford.
Siebecker, M.G., Li, W., Sparks, D.L., 2018. Chapter one - the important role of layered double hydroxides in soil chemical processes and remediation: what we have learned over the past 20 years. Adv. Agron. 147, 1–59.
Skovbjerg, L.L., Stipp, S.L.S., Utsunomiya, S., Ewing, R.C., 2006. The mechanisms of reduction of hexavalent chromium by green rust sodium sulphate: Formation of Cr-goethite. Geochim. Cosmochim. Acta 70, 3582–3592.
Taylor, R.M., Schwertmann, U., Fechter, H., 1985. A rapid method for the formation of Fe(II)Fe(III) hydroxycarbonate. Clay Miner. 20, 147–151.
Terry, N., Zayed, A.M., de Souza, M.P., Tarun, A.S., 2000. Selenium in higher plants. Annu. Rev. Plant Physiol. Plant Mol. Biol. 51, 401–432.
Trolard, F., Génin, J.R., Abdelmoula, M., Bourrié, G., Humbert, B., Herbillon, A., 1997. Identification of a green rust mineral in a reductomorphic soil by Mossbauer and Raman spectroscopies. Geochim. Cosmochim. Acta 61, 1107–1111.
Trolard, F., Bourrié, G., Abdelmoula, M., Refait, P., Feder, F., 2007. Fougerite, a new mineral of the pyroaurite-iowaite group: description and crystal structure. Clay Clay Miner. 55, 323–334.
Tsuji, M., 2002. SeO_3^{2-}-selective properties of inorganic materials synthesized by the soft chemical process. Solid State Ionics 151, 385–392.
Williams, A.G.B., Scherer, M.M., 2001. Kinetics of Cr(VI) reduction by carbonate green rust. Environ. Sci. Technol. 35, 3488–3494.
Williams, K.H., Wilkins, M.J., N'Guessan, A.L., Arey, B., Dodova, E., Dohnalkova, A., Holmes, D., Lovley, D.R., Long, P.E., 2013. Field evidence of selenium bioreduction in a uranium-contaminated aquifer. Environ. Microbiol. Rep. 5, 444–452.
Xu, Y., Dai, Y., Zhou, J., Xu, Z.P., Qian, G., Lu, G.Q., 2010. Removal efficiency of arsenate and phosphate from aqueous solution using layered double hydroxide materials: intercalation vs. precipitation. J. Mater. Chem. 20, 4684–4691.
Yang, L., Shahrivari, Z., Liu, P.K.T., Sahimi, M., Tsotsis, T.T., 2005. Removal of trace levels of arsenic and selenium from aqueous solutions by calcined and uncalcined layered double hydroxides (LDH). Ind. Eng. Chem. Res. 44, 6804–6815.
You, Y., Vance, G.F., Zhao, H., 2001. Selenium adsorption on Mg–Al and Zn–Al layered double hydroxides. Appl. Clay Sci. 20, 13–25.
Zhang, M., Reardon, E.J., 2003. Removal of B, Cr, Mo, and Se from wastewater by incorporation into hydrocalumite and ettringite. Environ. Sci. Technol. 37, 2947–2952.
Zingaro, R.A., Dufner, D.C., Murphy, A.P., Moody, C.D., 1997. Reduction of oxoselenium anions by iron(II) hydroxide. Environ. Int. 23, 299–304.